

Mechanical Stability of High-Molecular-Weight Polyacrylamides and an (acrylamido *tert*-butyl sulfonic acid)-Acrylamide Copolymer Used in Enhanced Oil Recovery

Abdul-Aziz Al-Hashmi,¹ Rashid Al-Maamari,¹ Ibtisam Al-Shabibi,¹ Ahmed Mansoor,¹ Hamed Al-Sharji,² Alain Zaitoun³

¹Department of Petroleum and Chemical Engineering, Sultan Qaboos University, 123 Muscat, Sultanate of Oman

²Petroleum Development Oman, 113 Muscat, Sultanate of Oman

³Poweltec, ZAC Rueil 2000, 92500 Rueil Malmaison, France

Correspondence to: A. A. Al-Hashmi (E-mail: azizra@squ.edu.om)

ABSTRACT: High-molecular-weight partially hydrolyzed and sulfonated polyacrylamides are widely used in enhanced oil recovery (EOR). Nonionic polyacrylamide and polyacrylamide-based microgels are also used in water shut-off treatments for gas and oil wells. A comparative study of the mechanical degradation for three linear polyacrylamides and a microgel is presented. Mechanical degradation is quantified from the loss of the viscosity of the polymer solution as it passes through a stainless steel capillary with a length of 10 cm and an internal diameter of 125 μm . The critical shear rate above which degradation increases exponentially was found to depend on the chemical structure of the polymer, molecular weight, and electrolyte strength. The nonionic polyacrylamide shows higher degradation and lower critical shear rate compared with a sulfonated polyacrylamide with similar molecular weight. Moreover, the nonionic polyacrylamide with a higher molecular weight results in lower mechanical degradation. The higher mechanical stability of the sulfonated polymer is attributed to the higher rigidity of its molecules in solution. On the other hand, the ability of the high-molecular-weight polymers to form transient, flow-induced microgels boost their mechanical stability. This ability increases with the increase in the molecular weight of the polymer. Indeed, the microgel solution used in this study demonstrates exceptional mechanical stability. In general, mechanical stability of linear polymers used in chemical enhanced oil recovery can be enhanced by tailoring a polymer that has large side groups similar to the sulfonated polyacrylamide. Also, polyacrylamide-based microgels can be applied if high mechanical stability is required. © 2014 Wiley Periodicals, Inc. *J. Appl. Polym. Sci.* **2014**, *131*, 40921.

KEYWORDS: copolymers; degradation; microgels; oil and gas; rheology

Received 23 December 2013; accepted 17 April 2014

DOI: 10.1002/app.40921

INTRODUCTION

Polyacrylamide-based polymers are widely used in water treatment,¹ paper manufacturing,² and enhanced oil recovery (EOR).³ In polymer EOR, high-molecular-weight polyacrylamides are used to increase the viscosity of the injected water for better oil displacement.³ The effectiveness of the polymer in increasing the water viscosity depends on the hydrodynamic radius of polymer chains in solution, which depends on its molecular weight (i.e., the end-to-end length of chain) at certain conditions of solvent type, temperature, and pH.³ Polymer chains can be irreversibly degraded through chain scission by mechanical, chemical, and biological mechanisms.^{3,4} The overall result of this degradation is a loss in the viscosifying power of the polymer; thus, the efficiency of the application is adversely affected.⁵ In polymer flooding, the initial degradation of the

polymer is due to mechanical degradation as a result of flow of polymer solution through pumps, flow lines, chokes, valves, and the flow through rock formation at the sand face.⁶ Such flow restrictions may induce high straining stress along the chain backbone, which can ultimately result in chain breakage.^{6–8} It was found that polymers experienced more than 65% loss of their initial viscosity as they flow from the injectors to the producers in field application.⁹

Another oilfield application of high-molecular-weight polyacrylamides is their use to reduce drag, hence decreasing the pumping cost of fluid transportation.^{10,11} Drag reduction of the polymer is adversely affected by scission of polymer molecules caused by the flow of the polymer through pumps, valves, and any other flow constriction (i.e., mechanical degradation).¹² Degradation can be also caused by repeated coil–stretch transitions experienced by

Table I. Chemical Composition of the Polymers Used as well as the Concentrations and the Viscosity of the Polymer Solutions Measured at 30°C and 10 s⁻¹

Polymer	MW (10 ⁶ g/mol)	% Hydrolysis/sulfonation	Concentration (mg/L)	μ_i (mPa.s)
NPAM06	6.5	<0.1	2700 (1% KCl)	10.0
			3000 (2% KCl)	14.0
NPAM18	18	<0.1	850 (2% KCl)	11.6
SPAM08	8	25	1600 (1% KCl)	13.0
			1800 (2% KCl)	11.4
M2ES		20	3500 (2% KCl)	15.2

the polymer in highly elongational turbulent flow systems.¹³ Hence, mechanical degradation of polymers used in drag reduction has recently received more attention.¹⁴

Chain's scission during elongational flow was predicted theoretically by the work of de Gennes¹⁵ due to the coil–stretch transition experienced by the polymer molecules. The coil–stretch transition is accompanied by a marked increase in the frictional contact between the stretched molecules and the solvent (i.e., marked increase in viscosity).¹⁵ In dilute polymer solutions, the rupture of macromolecules is anticipated in the mid-point of the fully stretched chain as has been demonstrated by the study of Keller and Odell.^{7,16} Flexibility of the polymer was found to play a crucial role in the coil–stretch transition.^{6,17} Flexibility enhancement due to higher molecular weight, substitution side groups, and salinity was found to increase polymer degradation.^{6,17} At high shear rates⁸ and elongational flow regimes through valves, chokes, and porous media, coils of high-molecular-weight polymers may open-up, possibly leading to subsequent chains' scission.

Mechanical degradation of EOR polymers was found to be partly responsible for lower efficiency in field applications.⁹ Degradation was found to be greater at the sand face.^{9,18} In capillary flow, polymer degradation occurs primarily at the entrance point where stretching of the macromolecules is maximum and extensional forces are sufficiently strong to cause bond scission.^{8,19,20} Degradation at the entry region of a capillary has been found to dominate above critical shear rate.⁸ The current study was conducted to evaluate the mechanical degradation of three high-molecular-weight polyacrylamides and a polyacrylamide-based microgel in order to investigate the effect of polymer chemical architecture and morphology. Polymer solutions were injected through 125- μm stainless steel capillaries. Mechanical degradation was measured by the drop in viscosity after injection. The behavior of the apparent viscosity of the polymer solutions during their flow through the capillary was also investigated to study the effect of polymer degradation on the solution apparent viscosity. The apparent viscosity can be calculated from pressure measurements during polymer solution flow compared with those measured during solvent flow in the capillary.

EXPERIMENTAL

Materials

Three linear polyacrylamides with different chemical structure were used. These polymers are two nonionic polyacrylamides (NPAM06 and NPAM18) and one sulfonated polyacrylamide (SPAM08). Table I lists the molecular weight and degree of sulfo-

nation provided by the manufacturer. NPAM06 and NPAM18 are linear nonionic polyacrylamides composed of acrylamide [Figure 1(a)]. SPAM08 is a sulfonated polyacrylamide with 25% sulfonation [i.e., 25% acrylamido *tert*-butyl sulfonic acid (ATBS) Figure 1(b) and 75% acrylamide]. The polyacrylamide-based microgel (M2ES) is an anionic polyacrylamide-based microgel composed of 80% acrylamide and 20% acrylate as shown in Figure 1(c). The nominal diameter of the M2ES is 2 μm , and it has a crosslinking density of 25 ppm using an organic crosslinker. All products were supplied by SNF Floerger (France). These polymers were dissolved in 1% or 2% KCl. Sodium azide (NaN_3) was added at a rate of 400 mg/L as a biocide for polymer long-term stabilization. All polymer solutions were prepared with viscosity values in the range 10–15.2 mPa.s at 10 s⁻¹ and 30°C. The concentration and initial viscosity of each solution at 30°C and 10 s⁻¹ are listed in Table I. A 10-cm long, 125- μm stainless steel capillary was used in capillary flow experiments.

Methodology

Preparation. The polymer solutions were prepared by slowly adding the polymer granules to the shoulder of a developed vortex of the solvent while maintaining vigorous stirring using a paddle mixer. The paddle speed was decreased after 1 h of polymer addition, and the polymer solution was left at room temperature thermostated at 20°C under slow mixing overnight to ensure complete dissolution.

Capillary Flow Experiments. The viscosity of the fresh polymer solutions was measured at 30°C using Bohlin Gemini Rheometer (Malvern) with double gap geometry (DG 24/27) in the shear rate range of 1–50 s⁻¹ in 5 min. The capillary flow measurements were started by solvent injection at 30°C using a syringe pump (ISCO, Model 100 DX). The solvent was injected at 1, 10, 25, 50, 100, 200, and 500 cm³/h through the capillary while measuring the pressure at stabilization, using a low-pressure transducer (Druck, 0–100 psi) for pressure values less than 100 psi and a high-pressure transducer for pressure values higher than 100 psi. This was followed by the injection of polymer solution at 30°C at increasing flow rates. The effluent was collected at each flow rate for viscosity measurement, which was conducted after 1 day of injection to permit sufficient time for polymer relaxation after being subjected to high shear stresses during capillary flow. The percentage of mechanical degradation (DR%) was calculated using the following equation⁶:

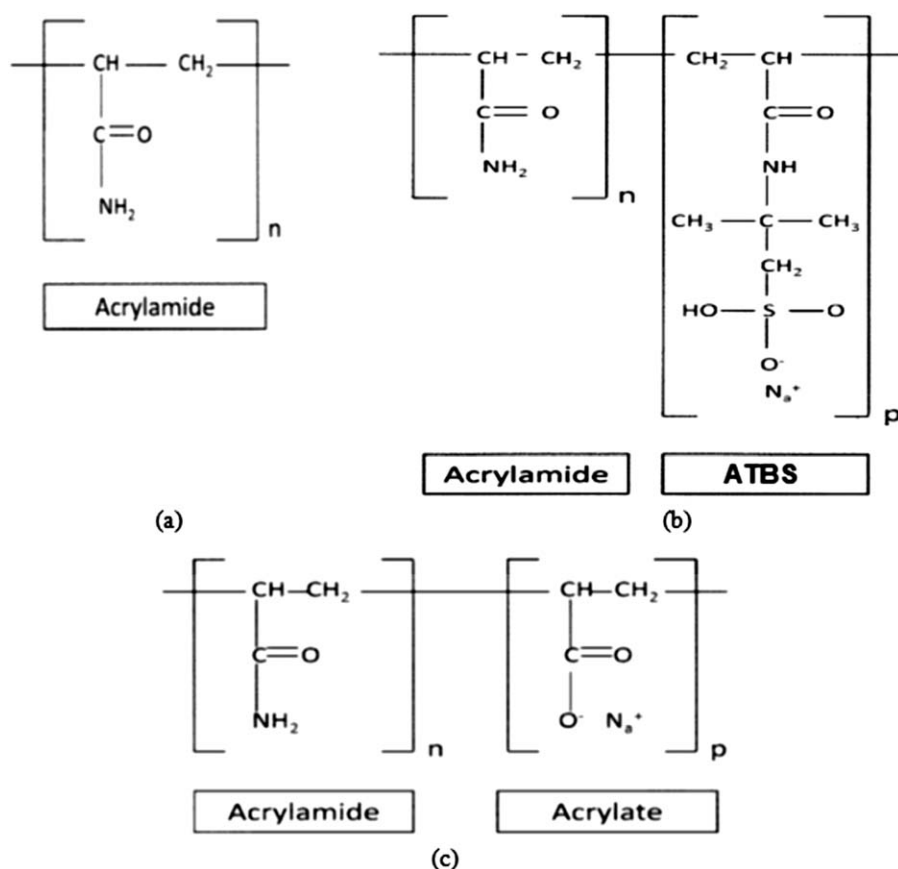


Figure 1. Chemical structure of the monomers composing the polymers.

$$DR(\%) = \left(\frac{\mu_{r0} - \mu_{rf}}{\mu_{r0} - 1} \right) \times 100\%$$

where, μ_{r0} is the initial relative viscosity and μ_{rf} is the relative viscosity of the effluent. All viscosities were compared based on a shear rate of 10 s^{-1} .

The tube diameter upstream the capillary entry point was with an internal diameter (D_{ent}) of 1.753 mm, which makes the contraction ratio of 14. Shear rate (γ) for a circular tube of radius (R) was calculated using the following equation²¹:

$$\gamma = \frac{4U}{R} = \frac{4Q}{\pi R^3}$$

where, U is the average velocity in m/s and Q is the volumetric flow rate in m^3/s .

The shear rate upstream the entry section is negligible compared with the shear rate inside the capillary. Hence, the shear rate in this work indicates its value inside the bulk of the capillary.

Mobility reduction (R_m) at a certain flow rate and constant temperature is defined by the following equation⁸:

$$R_m = \frac{\Delta P_p}{\Delta P_s} = \frac{\eta_p}{\eta_s}$$

where, ΔP_p is the pressure drop during polymer solution flow, ΔP_s is the pressure drop during solvent flow through fresh capillary, η_p is the apparent viscosity during polymer solution flow, and η_s is the viscosity of solvent.

The above equation is used to calculate the apparent viscosity of the polymer solutions at a certain flow rate inside the capillary by measuring the corresponding pressure drops. More details of the experimental procedure and experimental setup are in the recent work of Al-Hashmi et al.⁸

RESULTS AND DISCUSSION

Mechanical Degradation

The percentage of mechanical degradation calculated for the nonionic polyacrylamides (NPAM06 and NPAM18) is shown in Figure 2. Degradation of the sulfonated polymer (SPAM08) and the microgel (M2ES) is shown in Figure 3. Generally, linear polymers exhibited low degradation at low shear rates up to a critical shear rate, above which degradation starts to exponentially increase. The presence of an onset of mechanical degradation of polymer solutions has been found by other studies using different polymers.^{8,13,22} It has been found that the degradation below the critical shear rate is mainly due to shear inside the bulk of the capillary, whereas the elongation at the entry region is responsible for the sharp increase in degradation above the critical shear rate.⁸ The elongational flow through the abrupt contraction (i.e., at the entrance of the capillary) causes chains' scission due to high straining stress experienced by the polymer backbone above the critical shear rate.^{8,22–24}

The onset of mechanical degradation for SPAM08 in both 1% and 2% KCl is at a shear rate of $72,000 \text{ s}^{-1}$, which is about

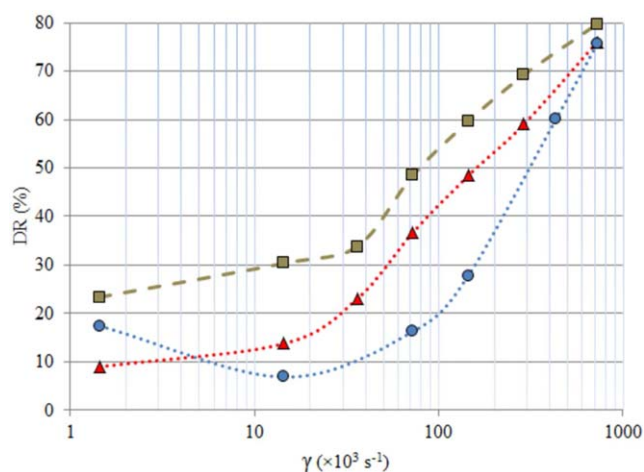


Figure 2. Polymer degradation of NPAM06 in 1% (\square) and 2% (Δ) KCl and NPAM18 in 2% KCl (\circ) as a result of solution flow through 10-cm long, 125- μ m stainless capillary, with contraction ratio of 14 at 30°C. [Color figure can be viewed in the online issue, which is available at wileyonlinelibrary.com.]

twice of that obtained for NPAM06 in 1% KCl and five times of that obtained in 2% KCl. Below the critical shear rate, the degradation of NPAM06 in 1% KCl is almost twice than that in 2% KCl. This might be due to the initial viscosity of NPAM06 in 2% KCl being 1.5 times of that in 1% KCl.

It has been found that shear (or mechanical) stability depends on the flexibility of the polymer in solution.⁶ The more rigid the polymer is in solution, the more resistant it is to mechanical degradation.⁶ This is validated in the current study by the higher critical shear rates for degradation for the sulfonated polyacrylamide (i.e., SPAM08) compared with the nonionic one (i.e., NPAM06). The sulfonated polyacrylamide owes its rigidity to the large, negatively-charged ATBS groups (ATBS is 313 \AA^3 and acrylamide 104 \AA^3).⁶ At the highest shear rate investigated in this study (i.e., 7.24×10^5 s $^{-1}$) degradation of SPAM08 was below 50%, whereas it was between 70% and 80% for NPAM06. The flexibility of charged polymers increases with the increase in electrolyte content, whereas nonionic polymers are generally not affected by electrolyte concentration. This is reflected by the lower slope of degradation increase above the critical shear rate for SPAM08 in 1% KCl solution compared with that in 2% KCl.

The higher-molecular-weight nonionic polyacrylamide (i.e., NPAM18) in 2% KCl exhibited higher mechanical stability, and the onset of degradation increase occurs at a critical shear rate of around 72,500 s $^{-1}$, which is twice of that obtained for NPAM06 in 2% KCl. Because the higher-molecular-weight polymer is more flexible, this result was not expected. However, this effect of molecular weight on polymer degradation is consistent with the results of other investigators.^{13,22} One of the possible explanations of this effect of molecular weight is the ability of the higher-molecular-weight polymers to form shear-induced entanglements between the polymer molecules.^{25–33} These microstructures (or shear-induced microgels) protect the chains from being individually subjected to the high straining stresses. This might also justify the lower degradation experienced by NPAM06 in 2% KCl compared with the 1% KCl solution. The concentration of NPAM06 in 2% KCl might give the polymer

more ability to form shear-induced microgel structures, hence giving it more mechanical stability. When compared with the mechanical degradation of a similar molecular weight partially hydrolyzed polyacrylamide,⁸ NPAM18 in 2% KCl is mechanically less stable. This is due to the more rigid conformation of the partially hydrolyzed polyacrylamide in 2% KCl due to the electrostatic repulsion between the negatively charged acrylate groups, which have comparable size with acrylamide.⁶

The microgel M2ES has shown higher stability than all linear polymers investigated. The critical shear rate for degradation for the microgel (M2ES) in 2% KCl is around 145,000 s $^{-1}$. There is initial decrease in microgel degradation to -10% (i.e., increase in effluent viscosity compared with the initial viscosity) between 72,500 and 145,000 s $^{-1}$. This is due to the possible presence of aggregates in the solution injected that are disintegrated by the flow through the capillary, hence increasing the effective viscosity of the solution. Another possibility for this increase in viscosity of the effluent is the damage caused to the internal structure of the microgel during flow through the capillary, hence allowing microgels to expand due to electrostatic repulsion between the negatively charged acrylate groups. Degradation of the M2ES at the highest shear rate investigated is around 10%, whereas the most stable linear polymer (SPAM08 in 1% KCl) has been degraded by around 37% at that shear rate. Hence, microgels tailored and manufactured with different sizes and cross-linking density^{34–36} can be alternatives for linear polymers in applications where high mechanical stability is required. These microgels have demonstrated superior mechanical and thermal stability compared with the linear polyacrylamides.³⁶

Effect of Polymer Degradation on the Apparent Viscosity

The apparent viscosity during the flow of the polymer solutions through the capillary is shown in Figures 4 and 5. All solutions exhibited an initial thickening followed by thinning above a critical shear rate. The critical shear rates for the thinning behavior for all linear polymer solutions is equal to those

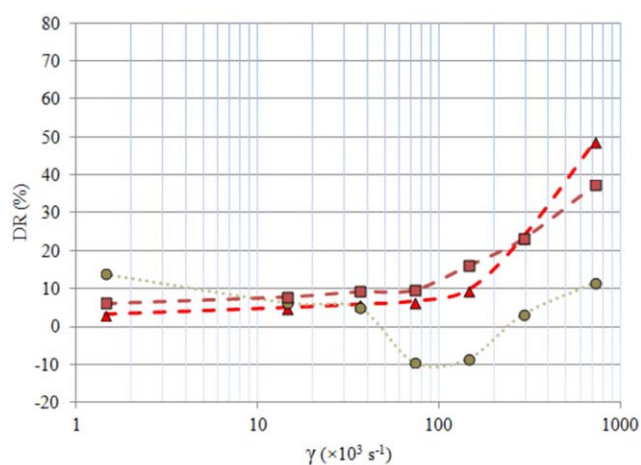


Figure 3. Polymer degradation of SPAM08 in 1% (\square) and 2% (Δ) KCl and M2ES in 2% KCl (\circ) as a result of solution flow through 10-cm long, 125- μ m stainless capillary, with contraction ratio of 14 at 30°C. [Color figure can be viewed in the online issue, which is available at wileyonlinelibrary.com.]

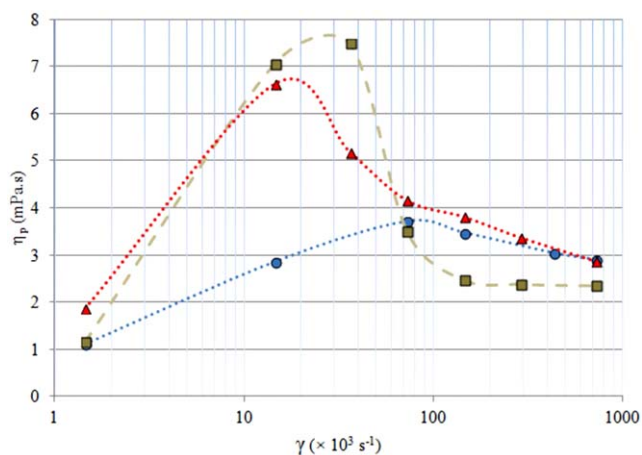


Figure 4. Apparent viscosity of NPAM06 in 1% (□) and 2% (Δ) KCl and NPAM18 in 2% KCl (○) as a result of solution flow through 10-cm long, 125- μm stainless steel capillary, with contraction ratio of 14 at 30°C. [Color figure can be viewed in the online issue, which is available at wileyonlinelibrary.com.]

obtained for the increase in mechanical degradation as listed in Table II. This indicates that the thinning behavior for the linear polymer solutions is due to increase in degradation above the critical shear rate.

The degree of thickening observed for NPAM06 in 1% KCl is higher than that for the same polymer in 2% KCl as shown in Figure 4. NPAM18 exhibited gradual thickening, reaching a maximum apparent viscosity of around 3.7 mPa.s at the critical shear rate of 72,500 s^{-1} . The maximum apparent viscosity of the lower-molecular-weight nonionic polyacrylamide (i.e., NPAM06) in 2% KCl is around 6.6 mPa.s at 14,500 s^{-1} . The thickening behavior of linear polymer solutions was mainly attributed to the elongation of individual polymer molecules.^{8,15,21,37–40} In a similar setup and using three different capillary lengths, Al-Hashmi et al.⁸ concluded that the thickening

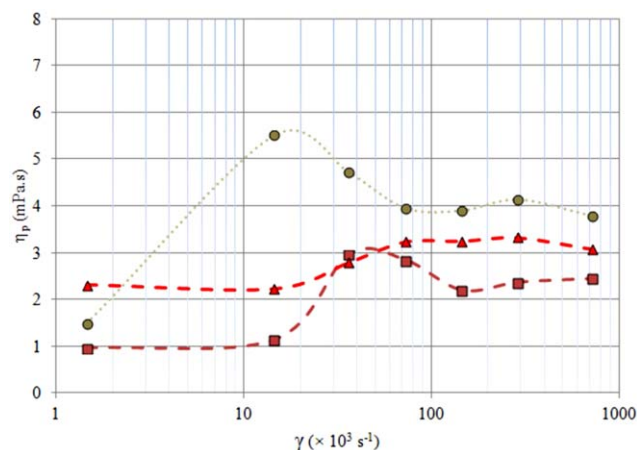


Figure 5. Apparent viscosity of SPAM08 in 1% (□) and 2% (Δ) KCl and M2ES in 2% KCl (○) as a result of solution flow through 10-cm long, 125- μm stainless steel capillary, with contraction ratio of 14 at 30°C. [Color figure can be viewed in the online issue, which is available at wileyonlinelibrary.com.]

Table II. Critical Shear Rate for Increase in Degradation and the Start of the Thinning Behavior

Polymer	Critical shear rate (s^{-1})	
	Degradation	Thinning behavior
NPAM06	36,000 (1% KCl)	36,000 (1% KCl)
	14,500 (2% KCl)	14,500 (2% KCl)
NPAM18	72,500 (2% KCl)	72,500 (2% KCl)
SPAM08	72,500 (1% KCl)	36,000 (1% KCl)
	145,000 (2% KCl)	No thinning
M2ES	145,000 (2% KCl)	14,500 (2% KCl)

behavior is due to extension of individual polymer molecules at the entry region of the capillary. Hence, more molecules per volume are being elongated for the lower-molecular-weight polymer, resulting in more thickening compared with the higher-molecular-weight one.

SPAM08 in 1% KCl exhibited low and almost constant apparent viscosity of around 1.0 mPa.s up to the shear rate of 14,500 s^{-1} , above which it increases to a maximum value of around 3.0 mPa.s at 36,000 s^{-1} before decreasing to a plateau of around 2.4 mPa.s. Similarly, SPAM08 in 2% KCl exhibited almost constant apparent viscosity at around 2.4 mPa.s up to the shear rate of 14,500 s^{-1} before increasing to a plateau value of around 3.2 mPa.s above 72,500 s^{-1} . The lower and flatter behavior of apparent viscosity with shear rate of the sulfonated polyacrylamide compared with that of the nonionic polyacrylamide is further supporting the higher rigidity of SPAM08. The extendibility of the sulfonated polymer at the capillary entrance is lower than that of the more coiled polymer chains of the nonionic polymer. The apparent viscosity of the microgel M2ES shows initial thickening, reaching a maximum value of around 5.5 mPa.s at 14,500 s^{-1} before decreasing to a plateau value of around 4.0 mPa.s above 72,500 s^{-1} . Because microgels do not elongate, the thickening of the M2ES is probably due to crowding of microgel aggregates at the entrance of the capillary, which is reduced at higher shear rates.

CONCLUSIONS

Mechanical degradation and apparent viscosity for different linear polyacrylamides and a polyacrylamide-based microgel were investigated by flowing polymer solutions at 30°C through 10-cm long, 125- μm stainless steel capillary. Polymer solutions with different concentrations in 1% KCl and 2% KCl were used to meet viscosity between 10 and 15.2 mPa.s at 30°C. The polymers were two nonionic polyacrylamides, a sulfonated polyacrylamide, and a 2- μm polyacrylamide-based microgel.

Mechanical degradation is constant at low shear rates until a critical shear rate is reached, above which a sharp increase in degradation is observed. The results show that mobility reduction increases until a critical shear rate is reached, above which it decreases to lower values. Generally, the critical shear rates for both increase in degradation and induction of thinning behavior are equal. This indicated that the thinning of the polymer solution during flow into the capillary is due to polymer degradation. Moreover, the mechanical stability of the polymer

is enhanced with a chemical structure of the linear polymer that gives it more rigidity. Also, degradation of the high-molecular-weight polymers can be reduced by their ability to form transient shear-induced microgels. Indeed, the microgel solution exhibited exceptional mechanical stability. This promotes microgels in chemical EOR applications that demand low loss of viscosity by mechanical degradation.

The initial thickening of the linear polymer solutions as they flow into a capillary is due to the elongation of the individual molecules. Above the critical shear rate at which degradation increases, polymer solutions exhibit thinning behavior due to chains' rupture at high straining stresses. On the other hand, the presence of aggregates in microgel solutions can be the reason of their initial thickening behavior.

ACKNOWLEDGMENTS

The authors thank the Petroleum Development Oman (PDO) for their financial support. This work was conducted as part of a joint R&D project between Sultan Qaboos University and Poweltec.

REFERENCES

1. Bolto, B.; Gregory, J. *Water Res.* **41** **2007**, *11*, 2301.
2. Wong, S. S.; Teng, T. T.; Ahmad, A. L.; Zuhairi, A.; Najafpour, G. *J. Hazard Mater.* **2006**, *135*, 378.
3. Sorbie, K. S. *Polymer Improved Oil Recovery*; Blackie: Glasgow-London, **1991**.
4. Caulfield, M. J.; Qiao, G. G.; Solomon, D. H. *Chem. Rev.* **2002**, *102*, 3067.
5. Tolstikh, L. I.; Akimov, N. L.; Golubeva, I. A.; Shvetsov, I. A. *Int. J. Polym. Mater.* **1992**, *17*, 177.
6. Zaitoun, A.; Makakou, P.; Blin, N.; Al-Maamari, R. S.; Al-Hashmi, A. R.; Abdel-Goad, M.; Al-Sharji, H. H. *SPEJ.* **2011**, *17*, 335.
7. Keller, A.; Muller, A.; Odell, J. *Prog. Colloid Polym. Sci.* **1987**, *75*, 179.
8. Al Hashmi, A. R.; Al Maamari, R. S.; Al Shabibi, I. S.; Mansoor, A. M.; Zaitoun, A.; Al Sharji, H. H. *J. Petrol. Sci. Eng.* **2013**, *105*, 100.
9. Wang, D.; Han, P.; Shao, Z.; Chen, J.; Seright, R.S. Sweep improvement options for the Daqing oil field. SPE 99441. Presented at the SPE/DOE Symposium on Improved Oil Recovery, Tulsa, OK, **2006**.
10. Sellin, R. H. J.; Hoyt, J. W.; Poliart, J.; Scrivener, O. *J. Hydraul. Res.* **1982**, *20*, 235.
11. Manfield, C. J.; Lawrence, C.; Hewitt, G. *Multiphase Sci. Tech.* **1999**, *11*, 197.
12. Liberatore M. W.; Baik, S.; McHugh, A. J.; Hanratty, T. J. *J. Non-Newton. Fluid Mech.* **2004**, *123*, 175.
13. Pereira, A. S.; Soares, E. J. *J. Non-Newton. Fluid Mech.* **2012**, *179*, 9.
14. Tabor, M.; deGennes, P. G. *Europhys. Lett.* **1986**, *7*, 519.
15. de Gennes, P. G. *J. Chem. Phys.* **1974**, *60*, 5030.
16. Keller, A.; Odell, J. A. *Colloid Polym. Sci.* **1985**, *263*, 181.
17. Odell, J. A.; Muller, A. J.; Keller, A. *Polymer* **1988**, *29*, 1179.
18. Seright, R. S. *SPEJ*, **1983**, *23*, 475.
19. Ghoniem, S.; Chauveteau, G.; Moan, M.; Wolff, C. *Can. J. Chem. Eng.* **1981**, *59*, 450.
20. Ghoniem, S. A. A. *Chem. Eng. Commun.* **1988**, *63*, 129.
21. Georgelos, P.; Torkelson, J. *J. Non-Newton. Fluid Mech.* **1988**, *27*, 191.
22. Moussa, T.; Tiu, C. *Chem. Eng. Sci.* **1994**, *49*, 1681.
23. Buchholz, B. A.; Zahn, J. M.; Kenward, M.; Slater, G. W.; Barron, A. E. *Polymer* **2004**, *45*, 1223.
24. Vanapalli, S. V.; Islam, M. T.; Solomon, M. J. *Phys. Fluids* **2005**, *17*, 095108.
25. Kishbaugh, A. J., McHugh, A. J. *Rheol. Acta* **1993**, *32*, 9.
26. Kishbaugh, A. J., McHugh, A. J. *Rheol. Acta* **1993**, *32*, 115.
27. Dupuis, D.; Lewandowski, F. Y.; Steiert, P.; Wolff, C. *J. Non-Newton. Fluid Mech.* **1994**, *54*, 11.
28. Saez, A. E.; Muller, A. J.; Odell, J. A. *Colloid. Polym. Sci.* **1994**, *272*, 1224.
29. Kauser, N.; Dos Santos, L.; Delgado, M.; Muller, A. J.; Saez, A. E. *J. Appl. Polym. Sci.* **1999**, *72*, 783.
30. Briscoe, B.; Luckham, P.; Zhu, S. *Rheol. Acta* **1999**, *38*, 224.
31. Torres, M. F.; Müller, A. J.; Sáez, A. E. *Polym. Bull.* **2002**, *47*, 475.
32. Al-Hashmi, A. R.; Luckham, P. F.; Grattoni, C. A. *J. Petrol. Sci. Eng.* **2013**, *112*, 1.
33. Vrahopoulou, E. P.; Mchugh, A. J. *J. Non-Newton. Fluid Mech.* **1987**, *25*, 157.
34. Frampton, H.; Morgan, J.; Cheung, S.; Chang, K.; Williams, D. Development of a novel waterflood conformance control system. SPE 89391. Presented at the SPE/DOE 14th Symposium on Improved Oil Recovery, Tulsa, OK, **2004**.
35. Cozic, C.; Rousseau, D.; Tabary, R. Novel insights into microgel systems for water control. SPE115974. Presented at the SPE Annual Technical Conference and Exhibition, Denver, CO, **2008**.
36. Dupuis, G.; Al-Maamari, R. S., Al-Hashmi, A. R., Al-Sharji, H. H.; Zaitoun, A. Mechanical and thermal stability of polyacrylamide-based microgel products for EOR. SPE 164135-MS. Presented at the 2013 SPE International Symposium on Oilfield Chemistry, The Woodlands, TX, **2013**.
37. Durst, F.; Haas, R.; Interthal, W. *Rheol. Acta* **1982**, *21*, 572.
38. Kulicke, W-M.; Hass, R. *Ind. Eng. Chem. Fundam.* **1984**, *23*, 308.
39. Stavland, A.; Jonsbranten, H. C.; Lohne, A.; Moen, A.; Giske, N. H. Polymer flooding—Flow properties in porous media versus rheological parameters. SPE131103. Presented at the EUROPEC/EAGE Annual Conference and Exhibition, Barcelona, Spain, **2010**.
40. Chauveteau, G.; Moan, M. *J. Non-Newton. Fluid Mech.* **1984**, *16*, 315.